Active Control of a Lightly Damped Cantilever Beam Using Spatially Distributed Actuators and Sensors

by

S. Sugavanam, B. V. Sankar
Department of Aerospace Engineering
Mechanics and Engineering Science
University of Florida
Gainesville, FL 32611

and

V. K. Varadan, V. V. Varadan
Department of Engineering Science and Mechanics
The Pennsylvania State University
University Park, PA 16802

ABSTRACT

This paper addresses the issue of active vibration control using bonded and embedded piezoceramic actuators and sensors. Two different piezoceramic actuator and sensor models are presented. The effect of actuator/sensor dynamics on the optimal placement of actuators and sensors is studied. A lightly damped cantilever beam is used to illustrate these ideas. It is shown that control effectiveness is maximized when the transducers are located at the root of the beam.

1 INTRODUCTION

In recent years there has been considerable interest in the use of bonded and embedded piezoceramic actuators and sensors for active vibration control Piezoceramic transducers effect vibration control by introducing "active electronic damping" to the structure. Several papers [1-9], have addressed the issue of modeling piezoceramic actuators and sensors. The optimal location of transducers for vibration control has been studied in [1,2,8].

Previously, the optimal placement of actuators and sensors has been studied in the context of centralized versus decentralized control. It has been reported that tip control is effective owing to the large response at the tip of the cantilever beam. On the other hand the simulations reported by Baz and Poh [2], and the experimental results of Hong et al [3], suggest that actuator effectiveness is maximized when the actuator is located near the clamped end of the beam. In order to better understand the problem of optimal location of sensors and actuators, the problem is addressed in the context of sensor/actuator dynamics.

This paper presents two different actuator and sensor models. The effect of transducer dynamics on the optimal location of actuators and sensors is studied. Simulation results are presented for the vibration control of a lightly damped cantilever beam. The results can be generalized for the control of large, flexible structures.

2 MODELING ISSUES

In this section, two approaches to modeling piezoceramic actuators and sensors are reviewed. The differences in the modeling are highlighted, as transducer effectiveness depends upon the underlying model. In Section 2.1, two sensor models are described. Sensor model A (SMA), describes the model employed by Hong et al, while sensor model B (SMB) describes the sensor as modeled by Hanagud et al. Similarly, in Section 2.2 the actuator model developed by Hong et al (AMA) and the actuator model developed by Hanagud et al (AMB) are presented.

2.1 Sensor Models

Model A

The sensor voltage generated by a piezoceramic sensor placed between locations $[x_{i-1}, x_i]$ on a uniform beam of width b, is given by

$$V_S(t) = -\left(\frac{Q_O}{C}\right)\int_{x_{i-1}}^{x_i}\left(\frac{\partial^2 W(x,t)}{\partial x^2}\right)dx \tag{1}$$

where Q_O is the charge coefficient, C is the capacitance of the piezoceramic sensor and $W(x,t)$ is the transverse displacement of the beam. On integration, the sensor voltage can be expressed as

$$V_S(t) = -\left(\frac{Q_O}{C}\right)\left[\left.\frac{\partial W(x,t)}{\partial x}\right|_{x=x_i} - \left.\frac{\partial W(x,t)}{\partial x}\right|_{x=x_{i-1}}\right]. \tag{2}$$

So, for SMA, the sensor voltage is proportional to the slope differential over the length of sensor. In[3], it has been shown that Eq. (2) can be approximated by

$$V_S(t) = -\left(\frac{Q_O}{C}\right)C^a(x_i)W(x_i,t) \tag{3}$$

where $C^a(x_i)$ is a constant that can be evaluated in terms of the slope-displacement ratios of the beam. This approximation is subject to the

Fig

assumptions that: (a) the sensors are short, (b) the sensors are placed near the root of the beam, (c) the neighboring modes give slope displacement constants of nearly the same value and (d) that each mode is equally weighted in the beam displacement as well as the beam slope. It follows that, if Eq. (3) is used to model the sensor voltage, then the sensor must be located near the root of the beam.

Model B

The one-dimensional constitutive equations for the piezoceramic material are given by

$$\begin{Bmatrix} \sigma_{11} \\ E_3 \end{Bmatrix} = \begin{bmatrix} C_{11} & -H \\ -H & \beta \end{bmatrix} \begin{Bmatrix} \varepsilon_{11} \\ D_3 \end{Bmatrix} \tag{4}$$

The above equation may also be written as

$$\begin{Bmatrix} \varepsilon_{11} \\ D_3 \end{Bmatrix} = \Delta \begin{bmatrix} \beta & H \\ H & C_{11} \end{bmatrix} \begin{Bmatrix} \sigma_{11} \\ E_3 \end{Bmatrix} \tag{5}$$

where $\Delta = \left(\beta C_{11} - H^2\right)^{-1}$, σ_{11} is the stress, ε_{11} is the strain, E_3 the electric field and D_3 is the charge per unit area. C_{11} is the elastic modulus under constant electric displacement, H the piezoelectric constant and β the dielectric constant under constant strain.

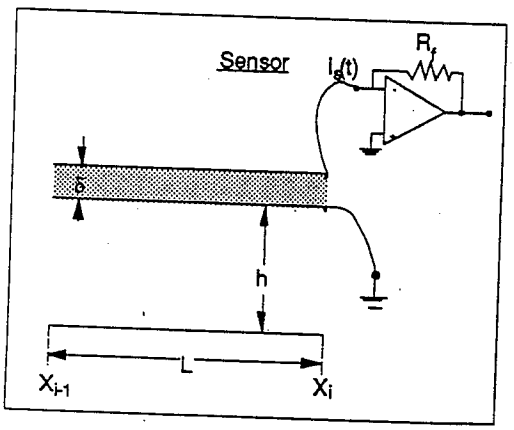

Figure 1

For the sensor configuration shown in Figure 1, the sensor is ideally a pure current source. In other words, for the zero impedance circuit shown, the second terms on the right-hand side of Eq. (5) are much smaller than the first terms on the same side of the equation. The sensor thickness is typically an order of magnitude smaller than the elastic beam height $2h$. Consequently, the strain distribution through the sensor cross section can be assumed to constant and equal to the upper fiber strain of the beam at $z = \pm h$. Thus for the sensor,

$$\varepsilon_{11} \approx D\beta\sigma_{11} = -hW''(x,t)$$
$$D_3 \approx \Delta H\sigma_{11} = -\beta^{-1}HhW''(x,t) \tag{6}$$

where ( )" denotes partial differentiation with respect to the variable x. Since the sensor current is proportional to the rate of charge developed,

$$i_s(t) = \int_{x_{i-1}}^{x_i} \dot{D}_3 b_s dx \tag{7}$$

where b_S is the width of the sensor and the overdot denotes partial differentiation with respect to time. The sensor is assumed to lie in the subdomain $x_{i-1}<x<x_i$, $z = h$. It follows that the sensor output voltage is given by

$$v_s = -R_f i_s(t) = b_s\beta^{-1}Hh\int_{x_{i-1}}^{x_i} \dot{W}''(x,t)dx \tag{8}$$

On integration the sensor output voltage can be expressed as

$$v_s = -k_s\left[\dot{\theta}_i - \dot{\theta}_{i-1}\right] \tag{9}$$

where $\dot{\theta}_i = \dot{W}(x,t)$ and $\dot{\theta}_{i-1} = \dot{W}(x_{i-1},t)$ and $k_s = R_f b_s\beta^{-1}Hh$.

It may be noted that in contrast to SMA, the sensor voltage in SMB is proportional to the differential of the time rate of the slope over the length of the sensor.

2.2 Actuator Models

Model A

The schematic for the piezoceramic actuator model employed by Hong et al is shown in Figure 2. The strain in the piezoceramic layer is given by

$$\varepsilon_{11} = \frac{d_{31}v_a}{\delta} \tag{10}$$

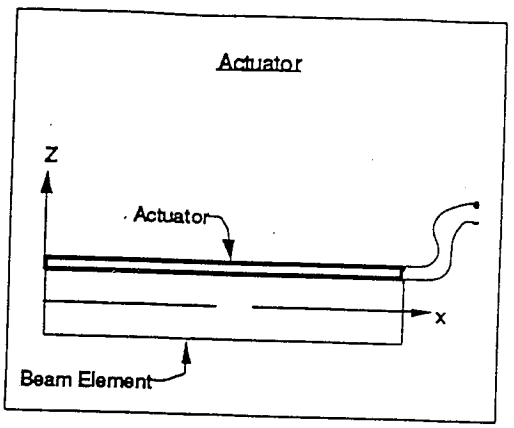

Figure 2

where d_{31} is the piezoelectric constant, δ the thickness of the piezoceramic layer and $v_a(t)$ the voltage applied to the piezoceramic actuator. The corresponding stress is given by

$$\sigma_{11} = E_p \frac{d_{31} v_a}{\delta} \tag{11}$$

where E_p is the elastic modulus of the piezoceramic material. This stress generates a bending moment about the neutral axis which may be expressed as

$$M_b = \int_h^{h+\delta} E_p \frac{d_{31} v_a}{\delta} b_a z dz \tag{12}$$

It then follows that the moment generated by the piezoceramic actuator is given by

$$M_b = E_p d_{31} v_a b_a \left(h + \frac{\delta}{2} \right) \tag{13}$$

It is seen that the moment generated by the piezoceramic actuator is directly proportional to the actuator voltage. Clearly, for an actuator of constant width b_a, the bending moment will be constant over the length of the actuator, and the bending moment diagram will be as shown in Figure 3. In [3], Hong et al use the idea of "equi-deflection" to relate the actuator voltage to a point load i.e. the moment M_b is replaced by a point load that produces an equivalent tip

deflection. When this is done, the corresponding point load F_a is related to the actuator voltage as

$$F_a \approx \frac{3}{2}\frac{E_p d_{31} b_a}{L_a}\left(h+\frac{\delta}{2}\right)v_a \tag{14}$$

where L_a is the length of the actuator. Thus in AMA, the actuator is modeled as a transducer producing a point force F_a in response to the actuator voltage v_a.

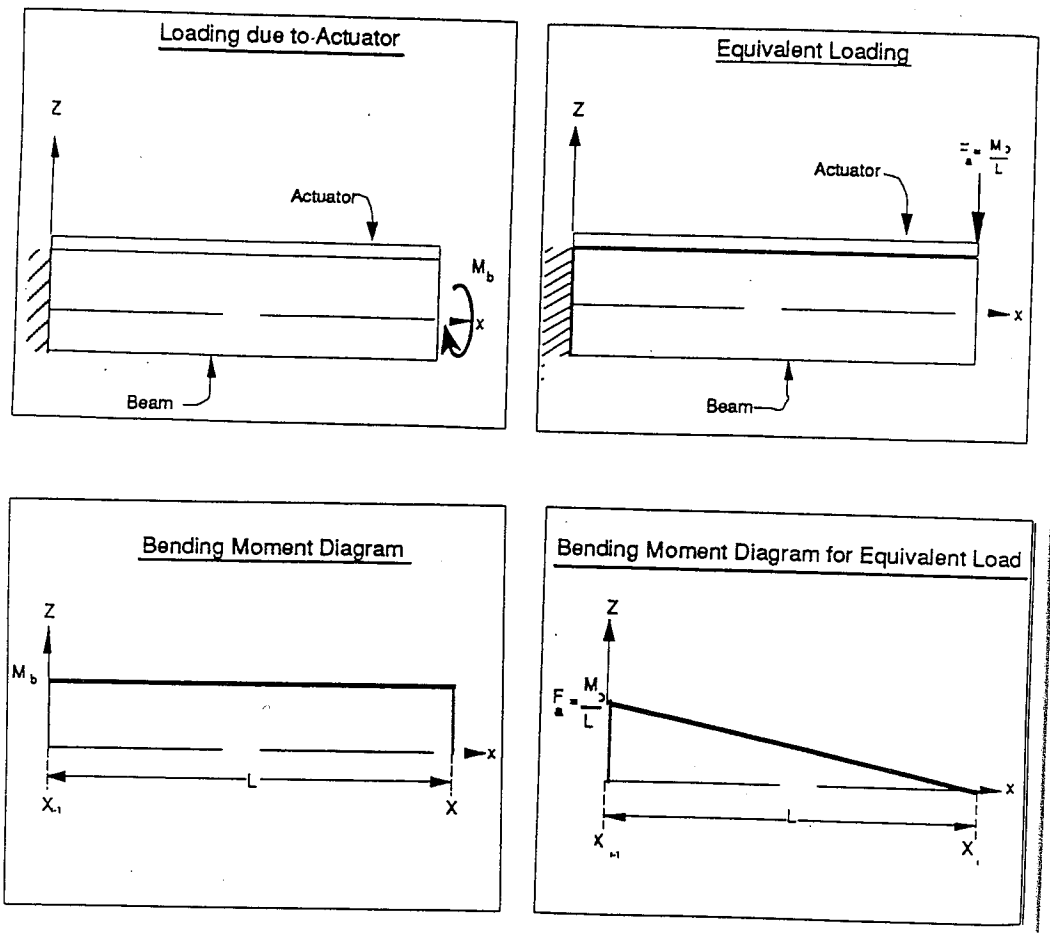

Figure 3

Model B

In [9], Hanagud et al model the piezoceramic actuator as follows. The voltage v_a generated by the actuator can be expressed as

$$v_a = \int_h^{h+\delta} E_3 dz \tag{15}$$

where E_3 is the electric field in the piezoceramic layer. Substituting for the electric field E_3, in terms of the constitutive equations in Eq. (4), it follows that

$$v_a = \int_h^{h+\delta} \left(-H\varepsilon_{11} + \beta D_3\right) dz \tag{16}$$

Since the thickness of the piezoceramic layer is much smaller than the height of the elastic beam, it is reasonable to assume that the strain distribution over the actuator cross section remains constant. It is also assumed that the electric displacement D_3 is constant over the actuator thickness i.e. $\frac{\partial D_3}{\partial z} = 0$. Rearranging Eq. (16) , and integrating it subject to these assumptions results in the following expression

$$D_3 = \frac{v_a(t)}{\beta\delta} + \frac{H\varepsilon_{11}}{\beta} \tag{17}$$

Substituting for the strain ε_{11} in the piezoceramic layer,

$$D_3 = \frac{v_a(t)}{\beta\delta} + \frac{H(h+0.5\delta)W''(x,t)}{\beta} \tag{18}$$

The stress in the layer is given by the constitutive equations in Eq. (4). Substituting for D_3 from Eq. (18), the stress in the actuator layer is given by

$$\sigma_{11} = \frac{-Hv_a}{\beta\delta} - \left(C_{11} - \frac{H^2}{\beta}\right)(h+0.5\delta)W''(x,t) \tag{19}$$

With this expression for the stress in the piezoceramic layer, the moment on the cross sectional face of the beam may be written as

$$M = EIW''(x,t) + \frac{\sigma_{11} I_a}{(h+0.5\delta)} \tag{20}$$

where I_a, which is the moment of inertia of the piezoceramic actuator, is given by

$$I_a = \frac{1}{12} b_a \delta^3 + (b_a \delta)(h + 0.5\delta)^2 \tag{21}$$

Substituting for I_a in Eq. (20) and once again, using the fact that $\delta << h$, yields the expression for the moment generated by the piezoceramic actuator

$$M - EIW''(x,t) = -\frac{Hb_a}{\beta}(h + 0.5\delta)v_a(t) \tag{22}$$

The similarity between Eqs. (22) and (13) should be noted. In both cases, the moment generated is proportional to $b_a\left(h + \frac{\delta}{2}\right)v_a(t)$. The signs can be adjusted by reversing the polarity of the voltage signal. In both cases, the moment generated by the piezoceramic actuator is directly related to the stress in the piezoceramic actuator. In the case of the cantilever beam with tip loading, the stresses are large near the root of the beam. This suggests that actuator effectiveness can be maximized by locating the piezoceramic actuator at the root of the beam.

The sensor models are however quite different. In the case of SMA, the sensor voltage is proportional to the slope differential over the length of sensor. However, in the case of SMB, the sensor voltage is proportional to the differential of the time rate of the slope over the length of the sensor. Consequently, the effectiveness of the sensor location may be different for the two sensor models. This issue will be addressed in the following section.

3. OPTIMAL CONTROL

The optimal control of a flexible structure using piezoceramic actuators and sensors is considered in this section. Consider a flexible structure embedded with piezoceramic actuators and sensors. The finite element model of the flexible structure is given by

$$M\ddot{q} + C\dot{q} + Kq = F^e + F^c \tag{23}$$

where M, C and K are the mass, damping and stiffness matrices. The external forces acting on the structure are denoted by F^e and the control forces exerted by the piezoceramic actuators are denoted by F^c.

In [9], Hanagud et al used an optimal output feedback procedure developed in [10] to determine the control gain matrix G. Here, structural control is effected using a linear quadratic regulator in conjunction with a

Kalman estimator. There are several reasons for using the LQG procedure as opposed to the optimal output feedback procedure. First, the optimal output feedback procedure is an iterative procedure. The procedure requires an initial guess at the control gain matrix G. This initial control gain must be chosen such that it stabilizes the system. Next, the iterative procedure may converge to a local minimum depending upon the choice of the initial control gain. Further, every iteration requires the solution of two Lyapunov equations, and this may be time consuming and computationally intensive as the size of the finite element model increases. Finally, [1] addressed the issue of centralized control versus decentralized control. On the other hand, the purpose here is to address the issue of optimal location of actuators and sensors.

In order to solve the control problem, the structural dynamic equations are cast in state space form as follows

$$\dot{x} = Ax + Bu + r$$
$$y = C_s x \tag{24}$$

where $x \in R^n$, $y \in R^r$,

$$A = \begin{bmatrix} 0 & I \\ -M^{-1}K & -M^{-1}C \end{bmatrix} \tag{25}$$

$$B = \begin{bmatrix} 0 \\ -M^{-1}K_D \end{bmatrix} \tag{26}$$

$$C_s = \begin{bmatrix} 0 & K_s \end{bmatrix} \tag{27}$$

$$x^T = \left\{ q^T \; \dot{q}^T \right\} \tag{28}$$

and

$$r^T = \left\{ 0 \; M^{-1} F^{eT} \right\} \tag{29}$$

Further,

$$K_D = \beta^{-1} H b_a h T_D \tag{30}$$

and

$$K_s = R_f \beta^{-1} H b_s h T_s \tag{31}$$

where T_D is the actuator location matrix and T_S is the sensor location matrix. In general, M, C and K correspond to a reduced order finite element model. The control gain is obtained by minimizing a quadratic performance index in the states and the controls

$$J = \int_0^\infty \left(x^T Q x + u^T R u \right) dt \tag{32}$$

The matrix Q is assumed to be positive semi-definite and the weighting matrix R associated with the control inputs is assumed to be positive definite. The control gain matrix G is given by

$$G = R^{-1} B^T S \tag{33}$$

where S is the solution to the steady state matrix Riccati equation

$$SA + A^T S - SBR^{-1} B^T S + Q = 0 \tag{34}$$

The control input is given by

$$u = -Gx \tag{35}$$

However, in general the state vector is not available for control and it is necessary to estimate the states using a Kalman filter. The Kalman filter estimates the states by minimizing the variance of the reconstruction error

$$E\left\{ \left[x(t) - \hat{x}(t) \right] \left[x(t) - \hat{x}(t) \right]^T \right\} \tag{36}$$

The states are estimated in terms of the Kalman filter gain as follows

$$\begin{aligned} \dot{\hat{x}} &= A\hat{x} + Bu + L\left(y - C_s \hat{x} \right) \\ y &= C_s x \end{aligned} \tag{37}$$

The Kalman gain L is given by

$$L = PC_s^T V^{-1} \tag{38}$$

where P is the solution to the steady state matrix Riccati equation

$$AP + PA^T + W - PC_s^T V C_s P = 0 \tag{39}$$

The matrices W and V correspond to the intensities of state excitation and observation noise. These processes are assumed to uncorrelated, zero mean, white noise processes. It is also assumed that the initial state of the system is uncorrelated with these noise processes.

The LQG controller implements the control in terms of the estimated control input $\hat{u} = -G\hat{x}$. The overall control system configuration is given by

$$\dot{x} = Ax + B\hat{u} + r$$
$$y = C_s x \tag{40}$$

$$\hat{u} = -G\hat{x}$$
$$\dot{\hat{x}} = (A - BG - LC)\hat{x} + Ly \tag{41}$$

This completes the description of the optimal control procedure for the structural vibration control problem. The open and closed responses of the structure are presented in the following section.

4. LOCATION OF ACTUATORS AND SENSORS

Consider an Euler-Bernoulli beam embedded with piezoceramic actuators and sensors. For the purpose of comparison, the cantilever beam example presented in [9] will be used here. The cantilever beam is 22.86 cm long and has cross-sectional dimensions of 1.65 x 0.44 cm. The beam is made of aluminum and is embedded with two piezoceramic transducers. The piezoceramic transducers are made of lead zirconate titanate (Gll95). The cross-sectional dimensions of the transducers are 1.65 x 0.0254 cm and the beam is subject to an impulse excitational the tip.

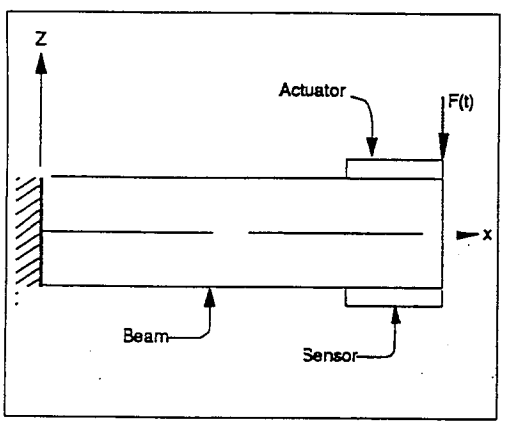

Figure 4

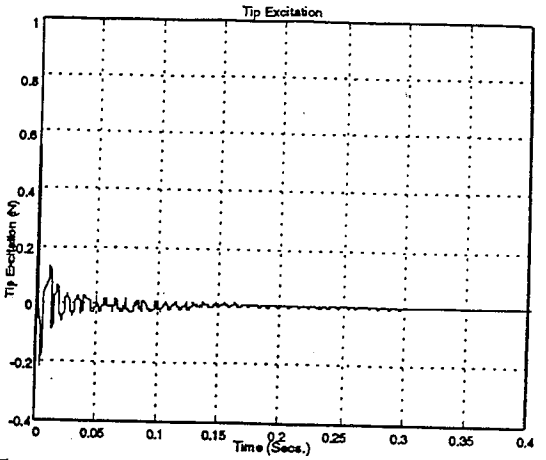

Figure 5

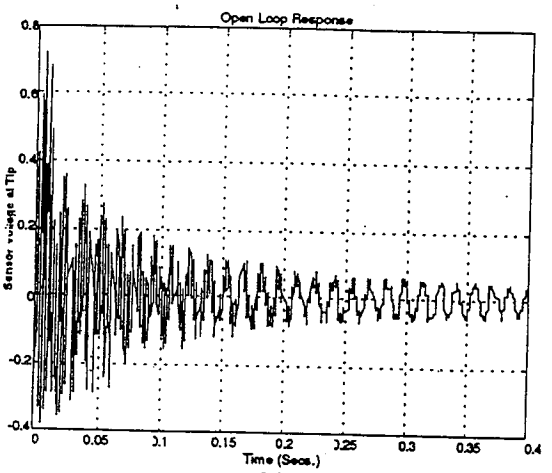

Figure 6

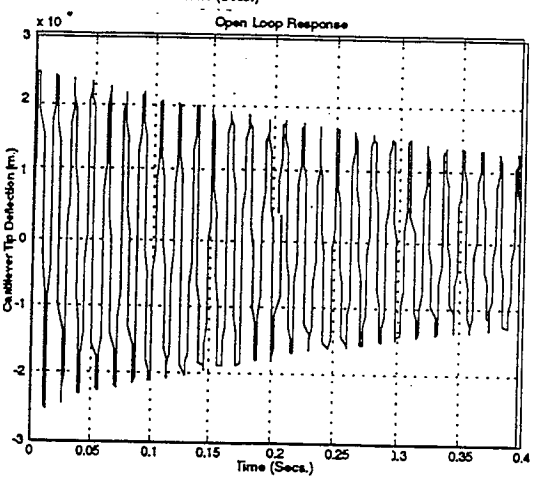

Figure 7

The mass and stiffness matrices for the cantilever beam shown in Fig. 4, are obtained using the finite element method. A modal damping factor of 0.004 is chosen for every mode. This is a typical value for thin, flexible structures [11]. [12]. It is assumed that the damping matrix is symmetric. The damping matrix is constructed using the first ten eigen values and eigen vectors and the modal damping factors. The beam is subject to the tip excitation shown in Fig. 5. The open loop response of the structure is shown in Fig. 6 and the transverse displacement of the tip of the cantilever beam is shown in Fig. 7.

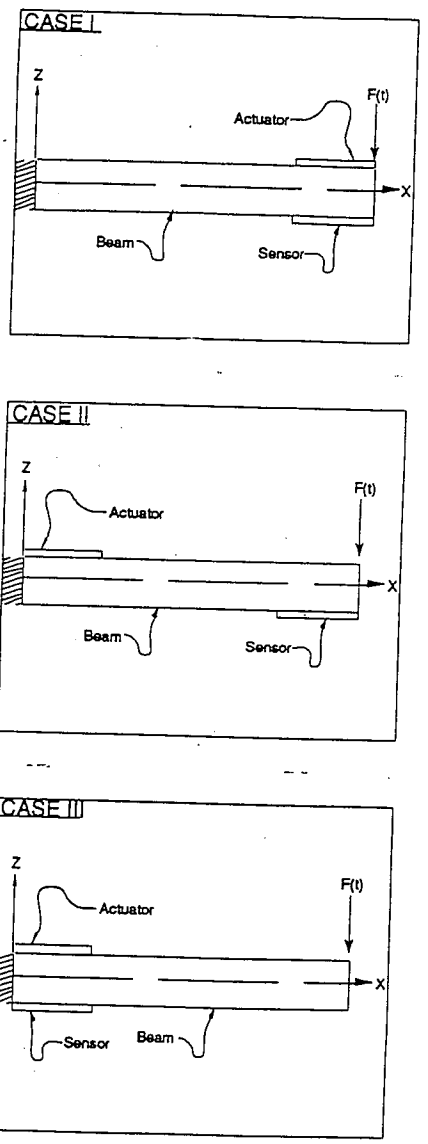

Figure 8

Three different actuator-sensor configurations are studied to understand the efficacy of actuator/sensor placement. The configurations are illustrated in Fig. 8. The simple LQG optimal control procedure presented in section 3 was used to determine the control and the Kalman filter gains. The state weighting matrix is chosen as follows:

$$[Q]=\begin{bmatrix} 1 & 0 & 0 & & \dots & 0 \\ 10^4 & 10^4 & 10^4 & & \dots & 10^4 \\ 0 & 0 & 1 & 0 & \dots & 0 \\ 10^4 & 10^4 & 10^4 & & \dots & 10^4 \\ & & & & & \\ 10^4 & 10^4 & 10^4 & & \dots & 10^4 \end{bmatrix} \tag{41}$$

The states associated with the θ_i and $\dot{\theta}_i$ are penalized heavily. This was done because in AMB, vibration control is effected by controlling the states $\theta_i(t)=\dfrac{\partial W(x_i,t)}{\partial x}$, i.e. the transverse deflection of the beam is controlled by applying control moments to the slope of the deflection. The control weighting matrix $[R]$ was set to $[I]$, the identify matrix. The intensity of the state noise $[W]$, is set to [5.5] based on the covariance of the tip excitation signal, and the observation noise intensity $[V]$, is set to $[I]$, the identity matrix, as the observation noise is assumed to be a zero-mean, Gaussian white noise process. The closed loop responses and the transverse displacement of the tip of the cantilever beam are presented in Figs. 9-14. Clearly, Case III represents the best closed-loop response.

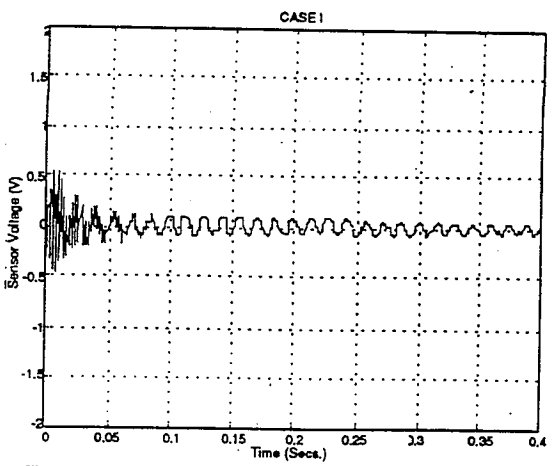

Figure 9

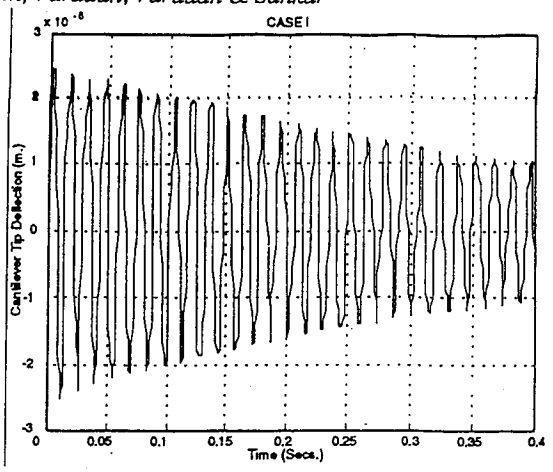

Figure 10

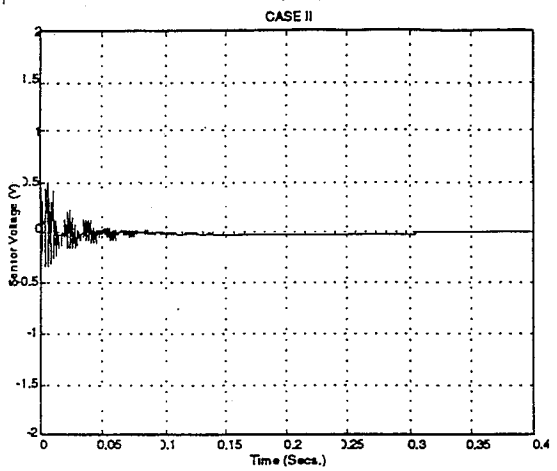

Figure 11

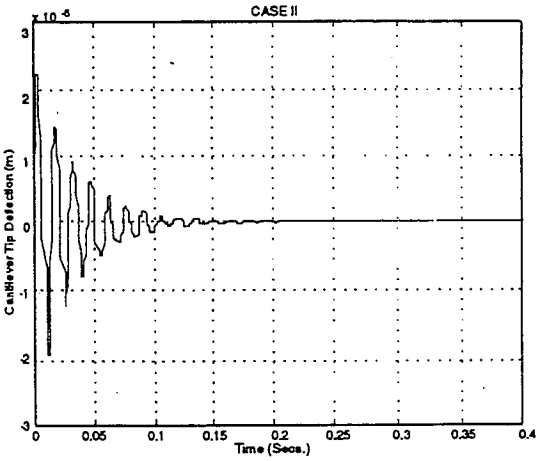

Figure 12

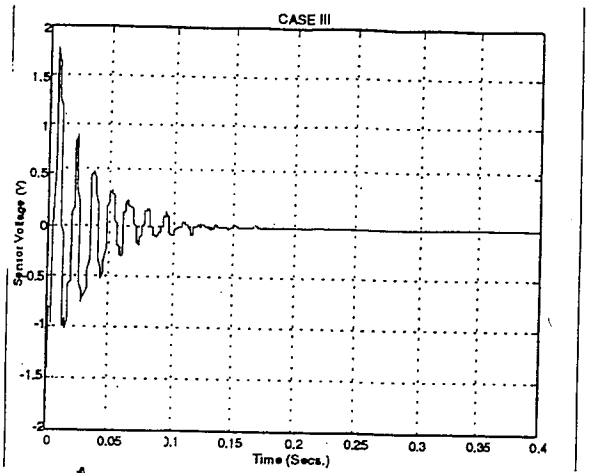

Figure 13

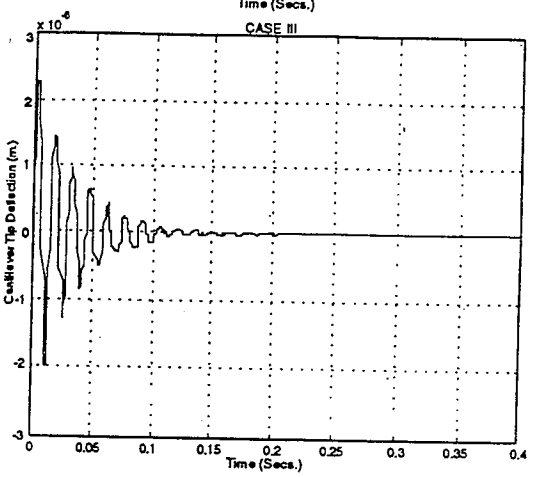

Figure 14

As anticipated in section 2, the efficacy of the actuator improves when the actuator is moved to the root end of the cantilever beam. This follows from a comparison of the closed loop response for Cases I and II. This result can be explained by the fact that the strains are large near the root of the beam. Consequently, a control voltage applied to the piezoceramic layer near the root of the beam, counteracts the strain at the point where the strain is largest. This is in agreement with the experimental results reported in [3]. Since, AMA and AMB are similar, the same reasoning applied to both the actuator models.

The issue of sensor efficacy is a little different. This is because SMA is quite different from SMB. In [3] , the sensor was located at the root of the cantilever beam owing to the assumptions involved in going from Eq. (2) to Eq. (3). In [1], it is suggested that the sensors and actuators be located at the tip of the cantilever beam, as the response at the tip of the cantilever beam is larger. From Fig. 15, it is seen that the response at the tip of the cantilever beam is indeed larger. However, a closer look at SMB reveals that the sensor voltage is

proportional to the differential of the time rate of the slope over the length of the sensor. A plot of the differential of the time rate of the slope over the length of the sensor (Fig. 16) for cases II and III, reveals that the sensor signal is much larger when the sensor is located at the root of the cantilever. It then follows that the actuator/sensor effectiveness is maximized when the actuator/sensor is placed at the root of the beam irrespective of the actuator/sensor model used. Similar results were obtained using the reduced order finite element model employed by Hanagud et al in [4].

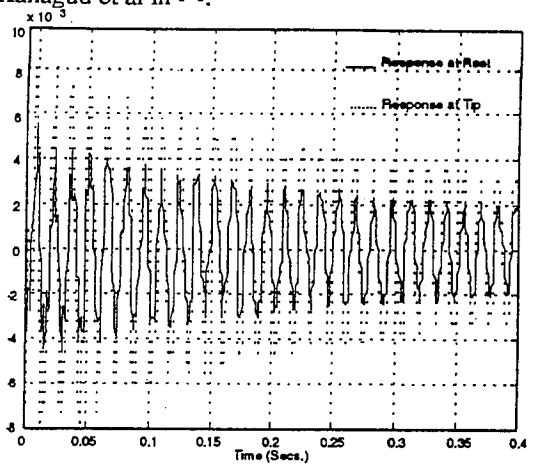

Figure 15

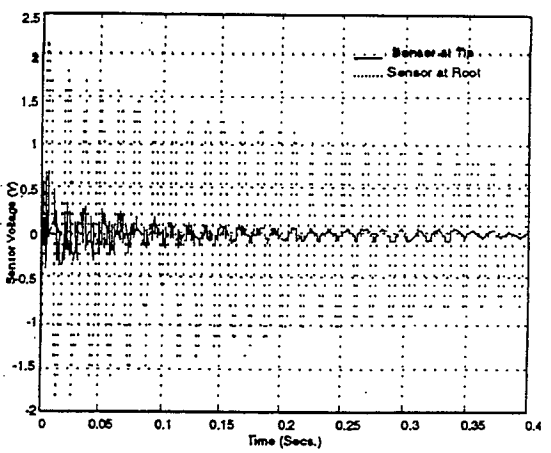

Figure 16

5. CONCLUSIONS

The optimal placement of piezoceramic actuators and sensors for structural control is considered. Two different approaches to modeling the actuators and sensors have been considered. In both cases it is shown that the effectiveness of the controller is enhanced when the actuator and sensor are placed

near the root of the beam. This is consistent with experimental results reported in the literature.

6. REFERENCE

1. S. Hanagud, C.C. Won and M. W. Obal, "Optimal Placement of Piezoceramic Sensors and Actuators," Proceedings of the American Control Conference, Vol. 3, 1988, pp. 1884-1889.
2. A. Baz, S. Poh, and P. Studer, "Optimum Vibration Control of Flexible Beams by Piezo-Electric Actuators".
3. S.-Y. Hong, V.V. Varadan and V. K. Varadan, "Comparison of Analog and Digital Strategies for Automatic Vibration Control of Lightweight Space Structures".
4. R. L. Forward and C. J. Swigert, "Electronic Damping of Orthogonal Bending Modes in a Cylindrical Mass," Journal of Spacecraft and Rockets, Vol. 18, No. 12, 1981, pp. 5-17.
5. E. F. Crawley, J. de Luis, N. W. Hagood and E. H. Anderson, "Development of Piezoelectric Technology for Applications in Control of Intelligent Structures," Proceedings of the American Control Conference, Vol. 3, 1988, pp. 1890-1896.
6. N. W. Hagood, W. H. Chung and A. von Flotow, "Modelling of Piezoelectric Actuator Dynamics for Active Structural Control" (AIAA Paper 90-1097)
7. T. Bailey and J. E. Hubbard, "Distributed Piezoelectric-Polymer Active Vibration Control of a Cantilever Beam," Journal of Guidance, Vol. 8, No. 5, Sep.-Oct. 1985, pp. 605-611.
8. J. de Lafontaine and M. E. Stieber, "Sensor/Actuator Selection and Placement for Control of Elastic Continua," IFAC Control of Distributed Parameter Systems, Los Angeles, CA, 1986, pp. 225-232.
9. S. Hanagud, M. W. Obal and A. J. Calise, "Optimal Vibration Control by the Use of Piezoceramic Sensors and Actuators," Journal of Guidance, Control and Dynamics, Vol. 15, No. 5, Sept.-Oct. 1992.
10. D. D. Moerder and A. J. Calise, "Convergence of a Numerical Algorithm for Calculating Optimal Output Feedback Gains," IEEE Transactions on Automatic Control, Vol. 30, No. 9, Sept. 1985.
11. J. E. Ruzicka, Structural Damping, ASME Colloquim on Structural Damping, Dec. 1959.
12. F. Hara, P. Y. Chen, S.S. Chen and A. G. Ware, "Damping - 1988", 1988 ASME Pressure Vessels and Piping Conference, June 1988.
13. H. Kwakernaak and R. Sivan, "Linear Optimal Control Systems," John Wiley and Sons, Inc., New York, NY 1972.
14. D. J Inman, "Vibration with Control, Measurement and Stability," Prentice Hall, Inc., Englewood Cliffs, NJ 1989.